Mutations in the Activation Loop Tyrosine of the Oncoprotein v-Fps†

Phillip Saylor, Ehab Hanna, and Joseph A. Adams*

Department of Chemistry, San Diego State University, San Diego, California 92182-1030

Received July 23, 1998; Revised Manuscript Received September 28, 1998

ABSTRACT: Mutations were made in the activation loop tyrosine of the kinase domain of the oncoprotein v-Fps to assess the role of autophosphorylation in catalysis. Three mutant proteins, Y1073E, Y1073Q, and Y1073F, were expressed and purified as fusion proteins of glutathione-S-transferase from *Escherichia coli* and their catalytic properties were evaluated. Y1073E, Y1073Q, and Y1073F have k_{cat} values that are reduced by 5-, 35-, and 40-fold relative to the wild-type enzyme, respectively. For all mutant enzymes, the K_m values for ATP and a peptide substrate, EAEIYEAIE, are changed by 0.4−2-fold compared to the wild-type enzyme. The slopes for the plots of relative turnover versus solvent viscosity [$(k_{cat})^{\eta}$] are 0.71 ± 0.08, 0.10 ± 0.06, and ≈0 for wild type, Y1073Q, and Y1073E, respectively. These results imply that the phosphoryl transfer rate constant is reduced by 19- and 130-fold for Y1073E and Y1073Q compared to the wild-type enzyme. The dissociation constant of the substrate peptide is 1.5−2.5-fold lower for the mutants compared to wild type. The inhibition constant for EAEIFEAIE, a competitive inhibitor, is unaffected for Y1073E and raised 3-fold for Y1073Q compared to wild type. Y1073E and Y1073Q are strongly activated by free magnesium to the same extent and the apparent affinity constant for the metal is similar to that for the wild-type enzyme. The data indicate that the major role of autophosphorylation in the tyrosine kinase domain of v-Fps is to increase the rate of phosphoryl transfer without greatly affecting active-site accessibility or the local environment of the activating metal. Finally, the similar rate enhancements for phosphoryl transfer in v-Fps compared to protein kinase A [Adams et al. (1995) *Biochemistry 34*, 2447−2454] upon autophosphorylation suggest a conserved mechanism for communication between the activation loop and the catalytic residues of these two enzymes.

Protein kinases direct cellular processes by controlling the phosphorylation level of target proteins. The addition of phosphoryl groups by protein kinases to key target proteins can affect metabolism, differentiation, secretion, DNA transcription, and cell division in the normal cell. Accordingly, protein kinases are strictly regulated in the cell by several mechanisms, including phosphorylation. Most protein kinases have a reversible phosphorylation site in the kinase domain that strongly activates catalytic function. Phosphorylation may be catalyzed by the same enzyme (autophosphorylation) or by another protein kinase. For example, cyclin-dependent protein kinases initiate progression through the cell cycle only when they are phosphorylated by another protein kinase in a critical loop region in the kinase domain known as the activation loop (*1*−*4*). This loop, located outside the active site, connects two β strands in the large lobe of the kinase domain. It is thought, on the basis of the X-ray structures of the phosphorylated and unphosphorylated forms of two protein kinases, cdk2, a cyclin-dependent kinase (*5*−*7*), and the insulin receptor kinase (IRK)[1] (*8*, *9*), that this loop is mobile when nonphosphorylated, occludes the substrate cavity, thereby prohibiting access to the active site, and alters the positioning of several key catalytic residues. These catalytic residues include a conserved aspartic acid in the DFG loop, which chelates the two metal ions, and a conserved glutamic acid, which forms an electrostatic interaction with a conserved lysine, fixing the nontransferable phosphates of ATP.

We have previously shown, using site-directed mutagenesis and detailed kinetic analyses, that autophosphorylation in the catalytic subunit of PKA has significant effects on two events in the catalytic cycle: ATP binding and phosphoryl transfer (*10*). Surprisingly, no mutations in Thr-197, the phosphorylation site in the activation loop, influence the binding affinity of substrate. While the structural studies on IRK and cdk2 indicate that phosphorylation should assist substrate binding, the kinetic results with PKA contradict these findings. Since no three-dimensional structure for the nonphosphorylated form of PKA is available, it is possible that the activation loop of PKA behaves differently than those for IRK and cdk2. Alternatively, the X-ray structures for these two protein kinases may not depict correctly the orientation of the activation loop in solution when nonphos-

† This work was supported by an NIH grant (CA 75112) and by the California Metabolic Research Foundation.

* To whom correspondence should be addressed: Telephone (619) 594-6196; Fax (619) 594-1879; E-mail jadams@sundown.sdsu.edu.

[1] Abbreviations: cdk2, cyclin-dependent kinase 2; FGFR, fibroblast growth factor receptor tyrosine-specific protein kinase; GST, glutathione-S-transferase; GST−kin, fusion protein of the kinase domain of v-Fps and glutathione-S-transferase; IRK, kinase domain of the insulin receptor; Mops, 3-(*N*-morpholino)propanesulfonic acid; PKA, cAMP-dependent protein kinase; TPK, tyrosine-specific protein kinase; v-Fps, nonreceptor tyrosine-specific protein kinase and transforming agent of the Fujinami sarcoma virus; Y1073E, Y1073F, and Y1073Q, glutathione-S-transfer−v-Fps kinase domain fusion proteins with tyrosine to glutamate, phenylalanine, and glutamine mutation, respectively, at position 1073.

10.1021/bi981775b CCC: $15.00
Published on Web 12/02/1998

phorylated. In support of this, the *B* factor for the activation loop in the nonphosphorylated cdk2 and other protein kinases is high, suggesting that this region of the protein is disordered in the crystal form.

To gain further insights into the role of phosphorylation in controlling the kinetic pathway for protein phosphorylation, we made several mutations in the activation loop of the kinase domain of the nonreceptor TPK, v-Fps. v-Fps is the oncogenic, retroviral product of the chicken c-Fps gene and has been shown to induce transformation in several cell lines including chicken embryo fibroblasts and Rat-2 cells (*11*−*13*). Most recently, it has been shown that the normal cellular forms of the Fps/Fes family are involved in the terminal differentiation of macrophages, making this enzyme family an important component of the immune response (*14*). We have expressed and purified a highly active, phosphorylated form of the kinase domain of v-Fps as a fusion protein of glutathione-S-transferase (GST) (*15*). This enzyme (GST−kin) is active toward exogenous peptide substrates and possesses a turnover number similar in value to that for PKA (*16*). We now report that removal of the phosphorylation site in the kinase domain of v-Fps primarily influences the rate of phosphoryl transfer without negatively affecting the binding affinity of the substrate or ATP or the local environment around the second, activating metal.

MATERIALS AND METHODS

Materials. Adenosine 5′-triphosphate (ATP), phosphoenolpyruvate, magnesium chloride, nicotinamide adenine dinucleotide, reduced (NADH), tris(hydroxymethyl)aminomethane (Tris), 3-(*N*-morpholino)propanesulfonic acid (Mops), pyruvate kinase type II from rabbit muscle, and lactate dehydrogenase type II from bovine heart were purchased from Sigma. Ethylenediaminetetraacetic acid (EDTA) and dithiothreitol (DTT) were purchased from Fisher. The restriction enzymes *Eco*RI and *Pst*I and elongase were purchased from Life Technologies, Stratagene, or New England Biolabs. Ultrapure agarose, cesium chloride, calf intestinal alkaline phosphatase, and T4 DNA ligase were purchased from Life Technologies. Ethidium bromide was purchased from Research Organics. Oligonucleotides were synthesized by Genset. DNA miniprep kits were purchased from Qiagen or Promega. The *Escherichia coli* strains BL21-(DE3) and SURE were purchased from Novagen and Stratagene, respectively.

Construction of Mutant Proteins. Mutants in the kinase domain of the v-Fps gene were made by PCR with a Perkin-Elmer T1 thermocycler, using four oligonucleotides for each mutation: two that define the ends of the kinase gene and two for the sites of mutation. The ends of the kinase gene were defined by the two oligonucleotides 5′-CGGGAATCAGCGGCCCATCACCCGCA-3′ and 5′-GATGAATTCCGTTTGCGG-3′. The three following sets of oligonucleotides were used to make the mutations: Y1073Q, 5′-GATGGTGTCCAGGCCTCCACG-3′ and 5′-CGTGGAGGCCTGGACACCATC-3′; Y1073E, 5′-GATGGTGTCGAGGCCTCCACG-3′ and 5′-CGTGGAGGCCTCGACACCATC-3′; and Y1073F, 5′-GATGGTGTCTTTGCCTCCACG-3′ and 5′-CGTGGAGGCAAAGACACCATC-3′. The PCR reactions were performed in a total volume of 50 μL with 60 mM Tris (pH 9.1), 18 mM $(NH_4)_2SO_4$ with 1.8 mM $MgSO_4$, 10 ng of template DNA, 0.2 mM of each dNTP, 1 unit of elongase, and 1 μM each primer. Primary PCR created the mutation while amplifying each half of the gene. Secondary PCR combined the two halves and amplified the entire mutant genes. The PCR products were ethanol-precipitated, dried, dissolved in TE buffer, and digested with *Eco*RI. The digested fragments were purified and ligated into the *Eco*RI site of pGEX-2T. The ligation products were transformed into a recombination-minus SURE strain of *E. coli*. Plasmid DNA from the putative clones was purified and the orientation of the inserted fragment was determined by a *Pst*I digestion. The correct clones were sequenced by the Sanger method (*29*) and then transformed into *E. coli* strain BL21-(DE3) for expression.

Peptides and Protein Purification. Peptide substrate, EAEIYEAIE, and inhibitor, EAEIFEAIE, were synthesized by the USC Microchemical Core Facility by using Fmoc chemistry and purified by C-18 reverse-phase HPLC. The concentration of the peptides was determined by weight. The fusion protein, GST−kin, was purified from *E. coli* by using a glutathione−agarose affinity resin according to previously published procedures (*15*, *16*) The total concentration of the protein was determined by a Bradford assay. While no free kinase domain is obtained from the affinity resin, free GST is observed as a breakdown product. The concentration of the fusion protein was determined by gel densitometry. Between 0.06 and 1.0 mg of fusion protein was obtained per 6 L preparation of *E. coli* cells. The enzyme was stored at −70 °C in a buffer containing 50 mM Tris (pH 7.5), 1 mM EDTA, 150 mM NaCl, 1 mM DTT, and 10% glycerol. The enzyme was thawed on ice (4 °C) and used immediately for each kinetic study.

Kinetic Assay. The enzymatic activity of GST−kin and the mutants were measured spectrophotometrically by a coupled enzyme assay. This assay couples the production of ADP with the oxidation of NADH by using pyruvate kinase and lactate dehydrogenase. In general, peptide (0.1−4 mM) was mixed manually with fixed ATP (2 mM), $MgCl_2$ (12.3 mM), and GST−kin (0.06−0.35 μM) in a 50 μL (minimum volume) quartz cuvette containing 0.40 mM phosphoenolpyruvate, 0.20 mM NADH, 2 units of lactate dehydrogenase, and 0.5 unit of pyruvate kinase. The total concentration of $MgCl_2$ needed to obtain a desired, free concentration of Mg^{2+} was calculated on the basis of the dissociation constants of 0.0143 mM for Mg-ATP, 5 mM for Mg-PEP, and 19.5 mM for Mg-NADH (*17*). All reactions were measured in a Beckman DU640 spectrophotometer equipped with a microcuvette holder in a buffer containing 50 mM Mops at pH 7.0, in a final volume of 60 μL at 23 °C. Background reactions in the absence of substrate peptide were performed to correct for ATPase activity. This background did not exceed 10% of the substrate-dependent reaction for wild-type or mutant enzymes. Absorbance changes at 340 nm were collected over a time range of 100−300 s. Less than 10% of the substrate peptide was consumed in each initial velocity measurement. All initial velocities varied linearly with the concentration of the fusion protein.

Viscosometric Measurements. The relative solution viscosities (η^{rel}) of buffers containing glycerol were measured relative to a standard buffer of 100 mM Mops, pH 7.0, at 23 °C, using an Ostwald viscometer (*18*). Each viscosity

Table 1: Steady-State Kinetic Parameters, Inhibition Constants, and Magnesium Dependencies for Wild-Type and Mutant Proteins[a]

	wild type	Y1073E	Y1073Q	Y1073F
k_{cat}[b] (s^{-1})	14 ± 2	3.0 ± 0.20 (5)	0.40 ± 0.10 (35)	0.33 ± 0.05 (40)
$K_{peptide}$[b] (mM)	0.43 ± 0.08	1.0 ± 0.16 (0.4)	0.50 ± 0.08 (0.8)	1.1 ± 0.30 (0.4)
K_I[b] (mM)	6.4 ± 0.70	9 ± 0.60 (0.7)	19 ± 3.0 (0.3)	
K_{ATP}[b] (mM)	0.22 ± 0.05	0.24 ± 0.05 (1)	0.10 ± 0.04 (2)	0.25 ± 0.10 (0.9)
v/v^0 [c]	13 ± 4.1	6.5 ± 1.7 (2)	13 ± 4.0 (1)	
K_{Mg}[c] (mM)	4.8 ± 1.0	5.1 ± 1.3 (0.9)	9.2 ± 1.2 (0.5)	

[a] All kinetic parameters were measured in 50 mM Mops buffer (pH 7) at 23 °C. The numbers in parentheses represent the ratios of the wild-type and mutant parameters. [b] These constants were measured in the presence of 10 mM free Mg^{2+} and fixed and variable levels of ATP, substrate, and inhibitor as stated in the text. [c] These parameters were derived from fitting the metal-dependent curves in Figure 2. v/v^0 is the ratio of the initial reaction velocity at infinite and zero concentrations of free Mg^{2+}, and K_{Mg} is the half-maximal concentration for these curves.

measurement was carried out in 5.0 mL of buffer containing varying amounts of viscosogen. The amount of time required for each buffer to move through the markings on the viscometer was recorded. The relative viscosity of each buffer was calculated from

$$\eta^{rel} = \frac{t(\%)}{t} \times \frac{\rho(\%)}{\rho} \quad (1)$$

where η^{rel} is the relative solvent viscosity, $t(\%)$ and t are the transit times for a given viscous buffer and the standard buffer, respectively, and $\rho(\%)$ and ρ are the densities of the viscous and standard buffers, respectively. The following relative solvent viscosities were obtained for the buffers (% viscosogen, η^{rel}): 35% glycerol, 3.7; 27% glycerol, 2.8; 20% glycerol, 2.1. All solvent viscosity measurements were performed in triplicate and did not deviate by more than 4% in value.

RESULTS

Steady-State Kinetic Parameters for Wild-Type and Mutant Proteins. The steady-state kinetic parameters for wild-type and mutant proteins were measured from plots of initial velocity (v) versus substrate peptide (EAEIYEAIE) or ATP concentrations by using the coupled enzyme assay in 50 mM Mops (pH 7) buffer. Plots of v versus peptide concentration at fixed ATP (2 mM) and 10 mM free Mg^{2+} (12.3 mM total $MgCl_2$) were used to measure k_{cat} and $K_{peptide}$ for wild-type GST−kin, Y1073E, Y1073F, and Y1073Q. Plots of v versus ATP concentration (0.03−3 mM) at 10 mM free Mg^{2+} (10.3−13.3 total $MgCl_2$) and fixed peptide concentrations (2 mM) were used to measure K_{ATP} for wild-type GST−kin, Y1073E, Y1073Q, and Y1073F. The results of these plots are shown in Table 1. For the wild-type enzyme, double-reciprocal plots of v versus substrate concentration at varied, fixed ATP intersect close to the x-axis (*16*), allowing an accurate measurement of K_{ATP} at subsaturating peptide concentrations. We have shown previously by comparing purified wild-type GST−kin and kin that GST does not influence the steady-state kinetic parameters (*15*). We have also shown that treatment of purified GST−kin with thrombin does not affect the specific activity of the enzyme (data not shown). These studies indicate that GST either as a fusion partner or free in solution does not influence the kinetic properties of the kinase domain.

All mutations have modest effects on the apparent affinities of ATP and the substrate peptide. With the exception of K_{ATP} for Y1073Q, the apparent dissociation constants (K_{ATP} and $K_{peptide}$) are raised no more than 2-fold relative to the wild-type enzyme. In contrast, turnover is lowered between 5- and 40-fold relative to the wild-type enzyme. Initial velocities used to determine all steady-state kinetic parameters varied linearly with the concentrations of the wild-type and mutant enzymes, indicating that the coupling reagents monitor the phosphorylation reaction. The values determined for wild-type v-Fps are consistent with previously measured values (*16*, *19*).

Inhibition of Wild-Type and Mutant Proteins by EAEIF-EAIE. Previous studies showed that the nine residue peptide EAEIFEAIE is a competitive inhibitor of GST−kin (*16*). The inhibitory constant (K_I) for EAEIFEAIE was measured for wild-type and two mutant proteins by a Dixon plot. Enzyme was preequilibrated with 2 mM ATP and varying amounts of inhibitor (0−20 mM) before the reaction was initiated with a fixed concentration of peptide substrate (0.5 mM). The total concentration of $MgCl_2$ was 12.3 mM (10 mM free Mg^{2+}). The true inhibition constants were then calculated from the apparent inhibition constant ($K_{I,app}$) by using the following relationship: $K_I = K_{I,app}/(1 + [S]/K_m)$. The values for wild-type and mutant proteins are given in Table 1. The K_I for wild-type GST−kin is consistent with a previously reported value of 4.6 mM (*16*). While the K_I value for Y1073Q is 3-fold higher than that for the wild-type enzyme, there is no significant change for Y1073E.

Viscosity Effects on the Steady-State Kinetic Parameters. The influence of glycerol on the steady-state kinetic parameters k_{cat} and $k_{cat}/K_{peptide}$ was measured for wild-type GST−kin and two of the mutant enzymes. For Y1073F, insufficient protein yields made it difficult to obtain a complete viscosity study. The initial velocity of the reaction was monitored as a function of peptide concentration (0.1−4 mM) with 2 mM ATP and 10 mM free Mg^{2+} (12.3 total $MgCl_2$) at varying percentages of glycerol in Mops buffer. In all cases, the initial velocities varied linearly with enzyme concentration, indicating that viscosogens did not adversely affect the ability of the coupling reagents to monitor peptide phosphorylation. The ratio of k_{cat} in the absence and presence of glycerol $[(k_{cat})^0/k_{cat}]$ for Y1073E, Y1073Q, and wild type is plotted as a function of relative solvent viscosity (η^{rel}) in Figure 1A. The ratio of $k_{cat}/K_{peptide}$ in the absence and presence of glycerol $[(k_{cat}/K_{peptide})^0/(k_{cat}/K_{peptide})]$ for Y1073E, Y1073Q, and wild type is plotted as a function of relative solvent viscosity (η^{rel}) in Figure 1B. These plots are linear with slope values $[(k_{cat})^\eta$ and $(k_{cat}/K_{peptide})^\eta]$ that are reported in Table 2. The slopes for wild type are similar to previously reported values (*16*, *19*). By comparison, the values of $(k_{cat})^\eta$ for the mutant enzymes are considerably lower than those observed

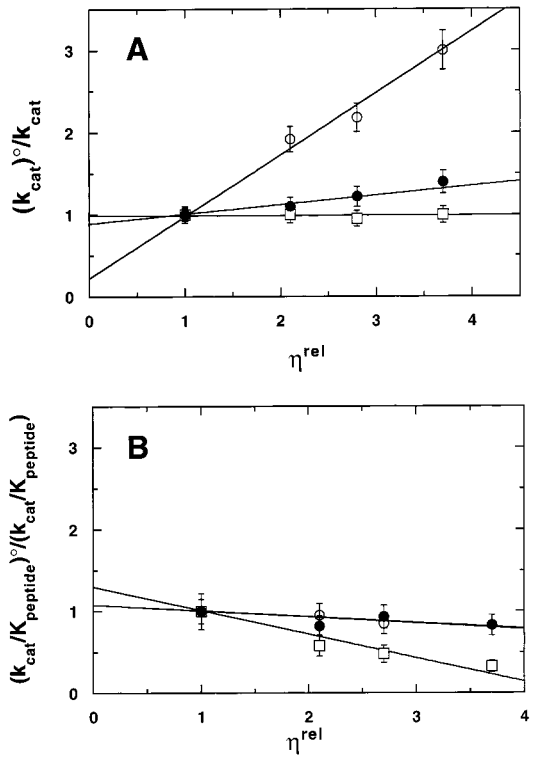

FIGURE 1: Effects of solvent viscosity on the steady-state kinetic parameters for wild-type enzyme (○), Y1073E (□), and Y1073Q (●). (A) Influence of viscosogens on k_{cat}. $(k_{cat})^0/k_{cat}$ is the ratio of k_{cat} in the absence and presence of varying glycerol and η^{rel} is the relative solvent viscosity. (B) Influence of viscosogens on $k_{cat}/K_{peptide}$. $(k_{cat}/K_{peptide})^0/(k_{cat}/K_{peptide})$ is the ratio of $k_{cat}/K_{peptide}$ in the absence and presence of varying glycerol concentrations and η^{rel} is the relative solvent viscosity. The values of k_{cat} and $k_{cat}/K_{peptide}$ were determined from plots of initial velocity versus peptide substrate concentration (0.1−4 mM) in the presence of 2 mM ATP and 10 mM free Mg^{2+}.

Table 2: Effects of Viscosity on the Steady-State Kinetic Parameters for Wild-Type and Mutant Proteins[a]

	wild type	Y1073E	Y1073Q
$(k_{cat})^{\eta}$ [b]	0.71 ± 0.08	0	0.10 ± 0.06
$(k_{cat}/K_{peptide})^{\eta}$ [b]	−0.07 ± 0.10	−0.29 ± 0.04	−0.065 ± 0.041
K_d(peptide)[c] (mM)	1.5 ± 0.49	1.0 ± 0.16 (1.5)	0.60 ± 0.041 (2.5)
k_3[d] (s^{-1})	48 ± 14	3 ± 0.2 (19)	0.44 ± 0.11 (130)
k_4[d] (s^{-1})	20 ± 3.6	≥30	4 ± 2.5 (5)

[a] All kinetic parameters were measured in 50 mM Mops buffer (pH 7) at 23 °C in the presence of 10 mM free Mg^{2+}. The numbers in parentheses represent the ratio of the wild-type and mutant parameters. [b] $(k_{cat})^{\eta}$ and $(k_{cat}/K_{peptide})^{\eta}$ are the slope values for plots of the steady-state kinetic parameters as ratios in the absence and presence of glycerol versus the relative solvent viscosities. These effects were measured from v vs substrate concentration (0.1−4 mM) plots at fixed concentrations of ATP (2 mM). [c] The K_d values for the peptide were measured by using eq 4. [d] The values of k_3 and k_4 were derived from the expression for the turnover number $[k_3k_4/(k_3 + k_4)]$ and $(k_{cat})^{\eta}$ by the following relationships: $k_4 = k_{cat}/(k_{cat})^{\eta}$ and $k_3 = k_{cat}/[1 - (k_{cat})^{\eta}]$ (*16*).

for the wild-type enzyme. While glycerol had no significant effect on $k_{cat}/K_{peptide}$ for Y1073Q or wild type, this viscosogen had an activating effect on this parameter for Y1073E (Table 2).

Magnesium Effects on the Reaction Rates for Wild-Type and Mutant Proteins. The influence of free Mg^{2+} concentration on reaction rates was measured for wild type, Y1073E, and Y1073Q to determine whether phosphorylation in the activation loop influences metal ion affinity. The relative velocity of the reaction was measured for the proteins under conditions of 1 mM ATP, 1 mM peptide substrate, and varying amounts of free Mg^{2+} (0.24−50 mM), and the results are shown in Figure 2. The velocity data are represented as relative rates since the mutants and wild-type enzymes have different specific activities. The data were fit to a hyperbolic function to obtain maximum and minimum rates at infinite and zero free Mg^{2+} and the apparent affinities (K_{Mg}) of the magnesium ion for the active sites of the proteins (Table 1). The ratio of the reaction velocity at infinite (v) and zero (v^0) free metal ion defines an activation parameter for the enzymes (v/v^0) that represents the ability of the second magnesium to enhance catalysis (*20*).

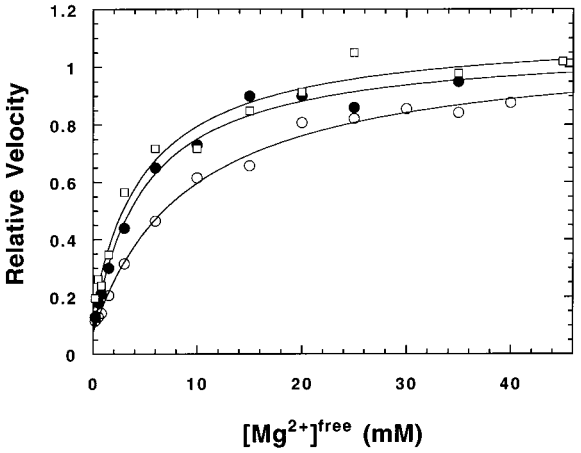

FIGURE 2: Effects of free Mg^{2+} concentration on the relative initial velocities for wild-type enzyme (●), Y1073E (○), and Y1073Q (□). The initial velocity is measured under conditions of 1 mM ATP and EAEIYEAIE and is represented as a relative velocity by normalizing the data to the velocity at infinite free Mg^{2+} concentrations. The total concentration range of $MgCl_2$ is 1.2−51 mM (0.24−50 mM free Mg^{2+}).

DISCUSSION

Many protein kinases are regulated by phosphorylation in the activation loop of the kinase domain. Prior studies have shown that Tyr → Phe substitution in the phosphorylation site in the activation loop of v-Fps leads to a 5-fold decrease in kinase activity as measured by an in vitro assay using immunoprecipitated protein and a buffer containing $MnCl_2$ (*21*). The identical mutation in c-Fes, the human cellular homologue of c-Fps, leads to a 10-fold decrease in catalytic activity (*22*, *23*). Despite these findings, the role of phosphorylation on individual steps in the kinase mechanism for either enzyme is uncharacterized with a physiological metal activator. Such detailed studies using several side-chain variations will elucidate the contributions of the phosphorylation site in this enzyme and put in perspective the general role of phosphorylation in protein kinase regulation. We showed previously that the phosphorylation of peptide substrates by v-Fps conforms to the kinetic mechanism shown in Scheme 1. At high ATP concentrations, the enzyme binds the substrate, EAEIYEAIE, with low affinity (k_{-2}/k_2 = 1.6 mM) and turnover is controlled by the rate of phosphoryl transfer (k_3 = 40 s^{-1}) and net product release (k_4 = 22 s^{-1}) (*16*). This mechanism now provides a solid framework for classifying the effects of site-specific mutations in this TPK.

Scheme 1

$$E\cdot ATP + S \underset{k_{-2}}{\overset{k_2}{\rightleftharpoons}} E\cdot ATP\cdot S \xrightarrow{k_3} E\cdot ADP\cdot P \xrightarrow{k_4}$$

Autophosphorylation Enhances Phosphoryl Transfer. Replacement of the phosphorylation site tyrosine in v-Fps with glutamic acid, glutamine, and phenylalanine reduces turnover by 5-, 35-, and 40-fold, respectively, without greatly impacting the apparent affinities of either ATP or substrate by more than 2.5-fold (Table 1). Since turnover is controlled by two steps in the wild-type enzyme (Scheme 1), we performed viscosity studies to determine the underlying cause of these reductions in k_{cat}. The turnover numbers for the mutants are more resistant to changes in solvent viscosity than that for the wild-type enzyme (Table 1 and Figure 1A). For wild type and Y1073Q no significant effect of solvent viscosity was observed on $k_{cat}/K_{peptide}$ (Figure 1B). By application of the Stokes−Einstein relationship, which equates diffusion coefficients and intrinsic viscosity, a direct correlation between the steady-state kinetic parameters, k_{cat} and $k_{cat}/k_{peptide}$, and the relative solvent viscosity of the medium can be made. Plots of either kinetic parameter as a ratio in the absence and presence of viscosogen versus relative solvent viscosity are linear and the slope values conform to

$$(k_{cat})^{\eta} = \frac{k_3}{k_3 + k_4} \quad (2)$$

$$(k_{cat}/K_{peptide})^{\eta} = \frac{k_3}{k_{-2} + k_3} \quad (3)$$

where $(k_{cat})^{\eta}$ and $(k_{cat}/K_{peptide})^{\eta}$ are the slopes for the plots of $(k_{cat})^0/k_{cat}$ and $(k_{cat}/K_{peptide})^0/(k_{cat}/K_{peptide})$ versus η^{rel}, respectively. Equations 2 and 3 predict that the slope values will fall between the limits of 0 and 1 where the former represents a viscosity-insensitive parameter and the latter represents a viscosity-sensitive parameter. We can use the rate expressions for k_{cat} $[k_3k_4/(k_3 + k_4)]$ and $k_{cat}/K_{peptide}$ $[k_2k_3/(k_{-2} + k_3)]$ and eqs 2 and 3 to determine the individual steps in Scheme 1.

By use of a viscosometric approach, the true effects of mutation on the steady-state kinetic parameters can be evaluated within the framework of Scheme 1. The lower effects of solvent viscosity on k_{cat} for the mutants compared to the wild-type enzyme imply that phosphoryl transfer is rate-determining when the enzyme is not phosphorylated (i.e., $k_3 < k_4$). Since phosphoryl transfer in the wild-type enzyme is only partially rate-determining, we conclude that the 5- and 35-fold reductions in turnover for Y1073E and Y1073Q are due to 19- and 130-fold reductions in k_3, respectively (Table 2). Insufficient protein yields for Y1073F made it difficult to obtain a detailed analysis of the effects of solvent viscosity on the kinetic parameters, but we presume that k_{cat} is limited primarily by phosphoryl transfer owing to the similar, low turnover numbers for this mutant and Y1073Q (compare 0.40 and 0.33 s^{-1} for Y1073Q and Y1073F and 14 s^{-1} for the wild-type enzyme; Table 1). Given this presumption, the phenylalanine substitution lowers the rate of phosphoryl transfer by 140-fold, a value similar to that for Y1073Q. While the net rate of product release is indeterminate for Y1073E since $(k_{cat})^{\eta} \approx 0$ (Table 2), there is a 5-fold reduction in this step for Y1073Q. Since we do not know, at this point, which step controls k_4, we currently treat it as a composite of several steps, which may include ADP or phosphopeptide dissociation or a conformational change. It is notable that the reduction in k_4 for Y1073Q is accompanied by a 2-fold increase in apparent ATP affinity (Table 1), possibly suggesting that ADP release may play a prominent role in controlling this step. For the catalytic subunit of PKA, a catalytic trapping technique was used to demonstrate that the rate-determining step in turnover is ADP release (*24*). Finally, the large reductions in $(k_{cat})^{\eta}$ for the mutants compared to the wild-type enzyme indicate that the effects on turnover (Table 1) represent true changes in mechanism rather than the presence of misfolded protein.

Autophosphorylation and Substrate Binding. The X-ray structures of cdk2 and IRK in both phosphorylated and nonphosphorylated forms suggest a steric role for the activation loops in the catalytic regulation of protein kinases (*5*−*9*). Phosphorylation of Thr-160 in cdk2 and trisphosphorylation of Tyr-1158, -1162, and -1163 in IRK cause substantial changes in the positioning of the activation loop. In the absence of phosphorylation, the loops appear to serve as autoinhibitory segments by occupying the active site and preventing substrate binding. Phosphorylation of the loop leads to an open active site that now permits substrate association. If the conclusions inferred from the analysis of these crystal structures can be applied in solution, then removal of the phosphorylation site in v-Fps should have significant, negative effects on the binding affinity of peptide substrates.

We tested this hypothesis by measuring the binding affinity of two nine residue peptides: a substrate, EAEIYEAIE, and an inhibitor, EAEIFEAIE. The dissociation constant for the substrate can be derived from the viscosity data in Table 2. With the exception of $(k_{cat}/K_{peptide})^{\eta}$ for Y1073E, the kinetic parameters fall within the limits predicted by eqs 2 and 3. The enhancement observed in $k_{cat}/K_{peptide}$ for Y1073E is due to decreases in $K_{peptide}$ at high viscosogens. Viscosogenic additives may improve peptide binding in this one case by stabilizing the ternary complex. However, we conclude, on the basis of the higher $K_{peptide}$ for this mutant and the lower value of k_{cat} compared to the wild-type enzyme, that the substrate is rapidly exchanging in the active site and $k_{cat}/K_{peptide}$ does not reflect the true association rate constant for the substrate. This is also true for wild-type enzyme and Y1073Q, on the basis of their low values for $(k_{cat}/K_{peptide})^{\eta}$ (Table 2). When $k_{-2} \gg k_3$, eq 4 can be used to determine the dissociation constant (K_d) for the peptide substrate to all proteins (Table 2):

$$K_{peptide} = K_d\,[1 - (k_{cat})^{\eta}] \quad (4)$$

This analysis indicates that neither mutation reduces the affinity of the substrate in the enzyme active site. In fact, Y1073Q binds the substrate 2.5-fold more tightly than wild type. If the slow step for Y1073F is phosphoryl transfer (i.e., $k_{-2} > k_3 < k_4$), then the K_d for the peptide is equivalent to $K_{peptide}$ for Y1073F, a value that is close to the calculated K_d for wild type (1.1 mM versus 1.6 mM; Table 1).

To gain further insights into the effects of autophosphorylation on the binding of the substrate to the kinase domain of v-Fps, we measured the binding affinity of a competitive inhibitor, EAEIFEAIE, to wild-type and mutant proteins.

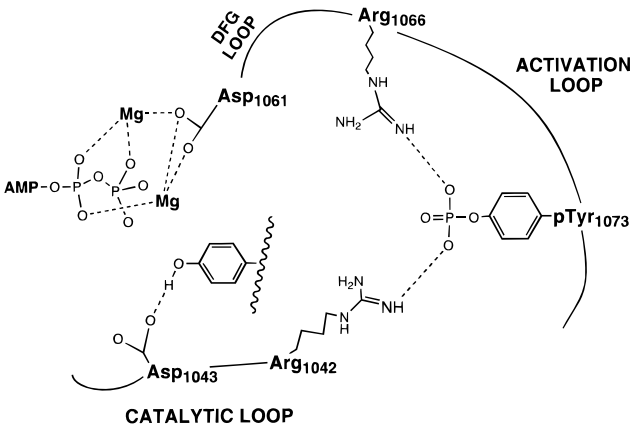

FIGURE 3: Predicted arrangement of several active-site residues in the kinase domain of v-Fps based on the X-ray structures of IRK and Lck (*9*, *25*). Arg-1066 and Arg-1042 are predicted to interact with pTyr-1073 in the activation loop. Asp-1061 chelates both metal ions and Asp-1043 forms a hydrogen bond with the phenolic group of the substrate.

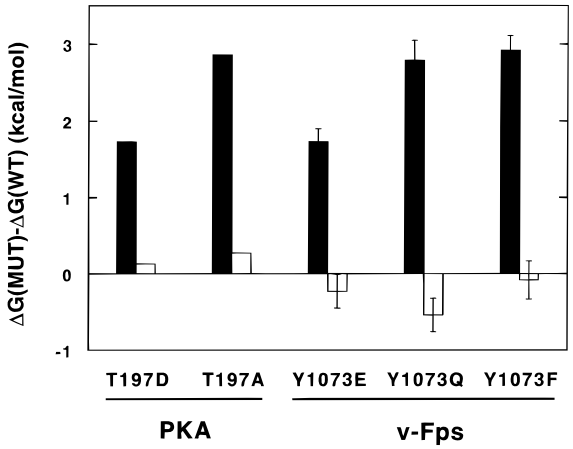

FIGURE 4: Effects of mutation in the phosphorylation site of the activation loops of the catalytic subunit of PKA and the kinase domain of v-Fps. The rates of phosphoryl transfer (solid bars) and the association constants ($1/K_d$) for the substrate peptides (open bars) are represented as the difference in free energy (ΔG) between the mutants and the wild-type proteins. The substrate peptides for v-Fps and PKA are EAEIYEAIE and LRRASLG. The data for PKA were taken from ref 10. It is assumed that k_{cat} and $K_{peptide}$ closely approximate k_3 and K_d for Y1073F (see text).

While substitution of tyrosine-1073 to glutamine has a 3-fold reduction in binding affinity compared to wild type, the glutamate substitution has no influence on inhibitor binding (Table 1). Although the former suggests that mutation has an effect on peptide binding, inherent differences in the substrate and inhibitor peptides may account for these subtle differences. The K_I for EAEIFEAIE to wild type is approximately 3-fold higher than the K_d predicted from the viscosity studies (Tables 1 and 2), suggesting that the additional hydrogen bond presented by the substrate is important for binding. In this regard, the inhibitor is not a perfect analogue for the substrate. Given these limitations, the binding data indicate that autophosphorylation has little effect on the binding of peptide substrates in the active site. These findings are consistent with those for the PKA autophosphorylation mutants where alanine and aspartate replacement of Thr-197 did not affect either K_d or K_I values for substrate or inhibitor (*10*).

Communication between the Activation Loop Tyrosine and the Active Site. The crystal structures of IRK and Lck suggest a potential mechanism for communication between the phosphorylation site and the active site in TPKs. In the active form of IRK, pTyr-1163 (Tyr-1073 in v-Fps) forms an electrostatic interaction with Arg-1155 (Arg-1066 in v-Fps), five residues C-terminal from the conserved aspartate in the DFG loop (*9*). This aspartate (Asp-1061 in v-Fps) is a ligand for both the primary and secondary magnesium ions, based on the IRK structure (*9*). In Lck, the analogous interaction is made in addition to a second electrostatic contact between the phosphotyrosine (pTyr-394) in the activation loop and Arg-363 (Arg-1042 in v-Fps), the first residue of the catalytic loop (*25*). While it is not clear why this second interaction is not made in IRK, there is a similar contact between the phosphothreonine in PKA and the first residue of the catalytic loop (*26*). Replacement of this residue in v-Fps (Arg-1042) with glutamic acid causes a 16-fold reduction in kinase activity, suggesting that a salt bridge may occur between this residue and pTyr-1073 (*27*). In the catalytic loop of IRK, the conserved aspartate (Asp-1043 in v-Fps) forms a hydrogen bond (2.7 Å) with the hydroxyl of the tyrosine substrate and may facilitate phosphoryl transfer through positioning or acid−base effects. Figure 3 shows a representation of several key amino acids in the active site of v-Fps and their connectivities to the activation loop and the phosphotyrosine, based on the available X-ray data from these related protein kinases. Consideration of this putative arrangement of amino acids in v-Fps suggests that regulation through phosphorylation may be linked to the active site through either the DFG or catalytic loops, with the former loop modifying catalysis through metal chelation.

To understand better how the phosphotyrosine in v-Fps can influence the rate of phosphoryl transfer by impacting the local environment of the active site, we measured the effects that the mutations have on metal-induced activity control. We have shown previously that the kinase domain of v-Fps is strongly activated by the binding of a second metal ion in the active site (*20*). On the basis of the IRK structure, this second metal should interact with the β phosphate of ATP and the conserved carboxylate of the DFG loop. If autophosphorylation affects positioning of Asp-1061 in the DFG loop of v-Fps (Figure 3), a potential source for the attenuations in phosphoryl transfer in the mutants, changes in the intrinsic affinity or activation parameters of the second metal would be expected. We measured the magnesium-dependent activation of wild-type and two mutant proteins and found them to be very similar (Figure 2). This implies that autophosphorylation does not influence the binding (K_{Mg}) or the activation parameters (v/v^0) of the metal. Such observations are consistent with an unaffected environment around this metal and suggest that catalytic control may not be linked to the DFG loop.

Conserved Features of Autophosphorylation. We have shown previously that mutation of Thr-197, the phosphorylation site in PKA, has a profound influence on phosphoryl transfer without affecting substrate binding (*10*). Figure 4 presents the mutational effects of Y1073 in v-Fps and compares them with those for T197 in PKA. Removal of the phosphoamino acid and replacement with a carboxylate side chain in either protein kinase leads to similar reductions in the rate of phosphoryl transfer with no changes in substrate affinity. While the Thr-197 → Ala and Tyr-1073 → Gln and

Phe substitutions do not depict isosteric replacements, they reduce phosphoryl transfer by similar amounts. We assert that the destabilization of phosphoryl transfer by approximately 3 kcal/mol in the latter group of mutations represents the true energetic contribution of autophosphorylation to catalysis for these two protein kinases.

The intermediate effects of T197D and Y1073E imply that the carboxyl can substitute partially for the phosphoamino acid. This substitution increases the energy barrier for phosphoryl transfer by only 1.5 kcal/mol compared to 3 kcal/mol for the less conservative replacements (Figure 4). Despite these similarities, it is important to note that this energetic penalty is not incurred by all protein kinases. For protein kinase C, replacement of the phosphothreonine in the activation loop with valine inactivates the enzyme, but glutamate substitution does not impair catalytic function (*28*). It is difficult to rationalize these results in light of those presented herein, but the presence of regulatory components and other neighboring subdomains in protein kinase C that are not present in the catalytic subunit of PKA or the kinase domain of v-Fps may influence the activation loop. Indeed, the binding of cyclin A to cdk2 causes a notable movement in the position of the activation loop, supporting this claim (*6*). Elucidation of the kinetic pathways for other protein kinases both with and without regulatory domains will define whether this phenomenon is conserved throughout the family of enzymes.

ACKNOWLEDGMENT

We thank Dr. Patricia Jennings for offering many useful suggestions regarding the manuscript.

REFERENCES

1. Gould, K. L., Moreno, S., Owen, D. J., Sazer, S., and Nurse, P. (1991) *EMBO J. 10*, 3297−3309.
2. Ducommun, B., Brambilla, P., Felix, M. A., Franza, B. R. J., Karsenti, E., and Draetta, G. (1991) *EMBO J. 10*, 3311−3319.
3. Solomon, M. J., Lee, T., and Kirschner, M. W. (1992) *Cell Regul. 3*, 13−27.
4. Morgan, D. O. (1995) *Nature 374*, 131−134.
5. Russo, A. A., Jeffrey, P. D., and Pavletich, N. P. (1996) *Nat. Struct. Biol. 3*, 696−700.
6. Jeffrey, P. D., Russo, A. A., Polyak, K., Gibbs, E., Hurwitz, J., Massague, J., and Pavletich, N. P. (1995) *Nature 376*, 313320.
7. DeBont, H. L., Rosenblatt, J., Jancarik, J., Jones, H. D., Morgan, D. O., and Kim, S. H. (1993) *Nature 363*, 595−602.
8. Hubbard, S. R., Wei, L., Ellis, L., and Hendrickson, W. A. (1994) *Nature 372*, 746−754.
9. Hubbard, S. R. (1997) *EMBO J. 16*, 5572−5581.
10. Adams, J. A., McGlone, M. L., Gibson, R., and Taylor, S. S. (1995) *Biochemistry 34*, 2447−2454.
11. Foster, D. A., Shibuya, M., and Hanafusa, H. (1985) *Cell 42*, 105−115.
12. Foster, D. A., and Hanafusa, H. (1983) *J. Virol. 48*, 744−751.
13. Feldman, R. A., Wang, E., and Hanafusa, H. (1983) *J. Virol. 45*, 782−791.
14. Areces, L. A., Sbarba, P. D., Jucker, M., Stanley, E. R., and Feldman, R. A. (1994) *Mol. Cell. Biol. 14*, 4606−4615.
15. Gish, G., McGlone, M. L., Pawson, T., and Adams, J. A. (1995) *Protein Eng. 8*, 609−614.
16. Wang, C., Lee, T. R., Lawrence, D. S., and Adams, J. A. (1996) *Biochemistry 35*, 1533−1539.
17. Martell, A. E., and Smith, R. M. (1977) *Critical Stability Constants*, Vol. 3, Plenum, New York.
18. Shoemaker, D. P., and Garland, C. W. (1962) *Experiments in Physical Chemistry*, 2nd ed.; McGraw-Hill, New York.
19. Adams, J. A. (1996) *Biochemistry 35*, 10949−10956.
20. Saylor, P., Wang, C., Hirai, T. J., and Adams, J. A. (1998) *Biochemistry 37*, 12624−12630.
21. Weinmaster, G., Zoller, M. J., Smith, M., Hinze, E., and Pawson, T. (1984) *Cell 37*, 559−568.
22. Hjermstad, S. J., Peters, K. L., Briggs, S. D., Glazer, R. I., and Smithgall, T. E. (1993) *Oncogene 8*, 2283−2292.
23. Fang, F., Ahmad, S., Lei, J., Klecker, R. W., Trepel, J. B., Smithgall, T. E., and Glazer, R. I. (1993) *Biochemistry 32*, 6995−7001.
24. Zhou, J., and Adams, J. A. (1997) *Biochemistry 36*, 15733−15738.
25. Yamaguchi, H., and Hendrickson, W. A. (1996) *Nature 384*, 484−489.
26. Zheng, J., Knighton, D. R., Ten Eyck, L. F., Karlsson, R., Xuong, N.-h., Taylor, S. S., and Sowadski, J. M. (1993) *Biochemistry 32*, 2154−2161.
27. Moran, M., Koch, A., Sadowski, I., and Pawson, T. (1988) *Oncogene 3*, 665−672.
28. Orr, J. W., and Newton, A. C. (1994) *J. Biol. Chem. 269*, 27715−27718.
29. Sanger, F., Nicklen, S., and Coulson, A. R. (1977) *Proc. Natl. Acad. Sci. U.S.A. 74*, 5463−5467.

BI981775B